

Lawrence Berkeley National Laboratory

Recent Work

Title

SURVEY OF INJECTION-SYSTEM DESIGN

Permalink

<https://escholarship.org/uc/item/5xj2k41j>

Author

Lamb, W.A.S.

Publication Date

1965-02-16

University of California

**Ernest O. Lawrence
Radiation Laboratory**

SURVEY OF INJECTION-SYSTEM DESIGN

TWO-WEEK LOAN COPY

*This is a Library Circulating Copy
which may be borrowed for two weeks.
For a personal retention copy, call
Tech. Info. Division, Ext. 5545*

Berkeley, California

DISCLAIMER

This document was prepared as an account of work sponsored by the United States Government. While this document is believed to contain correct information, neither the United States Government nor any agency thereof, nor the Regents of the University of California, nor any of their employees, makes any warranty, express or implied, or assumes any legal responsibility for the accuracy, completeness, or usefulness of any information, apparatus, product, or process disclosed, or represents that its use would not infringe privately owned rights. Reference herein to any specific commercial product, process, or service by its trade name, trademark, manufacturer, or otherwise, does not necessarily constitute or imply its endorsement, recommendation, or favoring by the United States Government or any agency thereof, or the Regents of the University of California. The views and opinions of authors expressed herein do not necessarily state or reflect those of the United States Government or any agency thereof or the Regents of the University of California.

Particle Accelerator Conference,
Washington, D. C. , March 10-12, 1965

UCRL-11955

UNIVERSITY OF CALIFORNIA

Lawrence Radiation Laboratory
Berkeley, California

AEC Contract No. W-7405-eng-48

SURVEY OF INJECTION-SYSTEM DESIGN

W. A. S. Lamb

February 16, 1965

SURVEY OF INJECTION-SYSTEM DESIGN*

W. A. S. Lamb

Lawrence Radiation Laboratory
University of California
Berkeley, California

February 16, 1965

Abstract

The general problems of injection into particle accelerators are discussed with the criteria for the choice of injection parameters emphasized. Examples are given of the injection system designed for a 200-BeV proton synchrotron.

Introduction

It is the function of an injection system to provide a charged-particle beam acceptable to the accelerator with minimum beam loss, and to represent a reasonable proportion of the cost of the entire accelerator. The as-yet undiscovered accelerator, which will efficiently and cheaply accelerate protons from the gas bottle to super-high energies without the services of any injection system, will remove many of the operational difficulties of present-day machines. A look at the design for the injection systems of the super-energy machines considered today is a partial review of the accelerator art. The beam is born in a Cockcroft-Walton column (circa 1931), goes next to a linear accelerator (2π standing-wave type, 1947), and finally to an alternating gradient synchrotron, for the moment the ultimate high-energy accelerators (1959).

Some of the criteria for the selection of the parameters of an injection system for a 200-BeV proton synchrotron, under study at the Lawrence Radiation Laboratory for the past 2 years, are discussed here. Although a specific system is discussed, it is hoped that the discussion will be general enough to be useful for other applications.

The design of an injection system starts with the choice of the type of machine to be utilized for a particular particle-energy range, and consequent optimization of the energies of transition from one type of machine to the other. Ignoring for the moment the other requirements, we see that the different types of proton accelerators have a wide variation in their cost per unit of energy gain. Listed below in order of increasing

cost per eV of energy gain are common general types of accelerators:

1. Proton synchrotron - alternating gradient (strong focusing)
2. Proton synchrotron - constant gradient (weak focusing)
3. Linear accelerator
4. dc Accelerator - Cockcroft-Walton

The injection system discussed here (shown diagrammatically in Fig. 1) consists of:

1. An ion source and dc accelerating column
2. An rf buncher
3. A 2π -mode standing-wave linear accelerator
4. A debuncher
5. A rapid-cycling alternating-gradient proton synchrotron.

Ion Source and Cockcroft-Walton Accelerator

The transverse-beam characteristics of the Cockcroft-Walton accelerator can be described by a phase area in several pairs of variables. Consider first the case of a beam defined by a pair of circular apertures of diameter $d = 2a$, which are spaced a distance l apart (Fig. 2).

If the angle is small ($\alpha \approx \tan \alpha$), the extreme angle transmitted by this simple system is

$$\alpha = 2a/l . \quad (1)$$

If we now consider the angle α as being due to the transverse momentum component p_x , we also have

$$\alpha = p_x/p_z . \quad (2)$$

This system of diaphragms (Fig. 2) has an "emittance" E "looking" into the beam or an "admittance" A "looking" from the source. The phase area is

*Work done under the auspices of the U. S. Atomic Energy Commission.

$$E = \pi a a = \pi \frac{p_x}{p_z} \cdot a \text{ rad-cm.} \quad (3)$$

The emittance area is that of an ellipse with semi-axes a and a . The area of this phase ellipse is conserved upon free-space drift or passage through optical systems, but its orientation can be changed. Matching emittance of one system to the admittance of another consists not only of making the area of the emittance phase space equal or slightly less than the admittance, but also having the proper orientation of the phase space ellipse in order to avoid "real" space obstacles such as the bore size in a drift tube. Figure 3 shows diagrammatically the behavior of the phase space ellipse.

If the beam is now accelerated in the z direction and p_x remains unchanged, the angle-displacement phase area is reduced and the beam will pass through a smaller diameter of defining apertures as its "quality" is improved. In order to have a description of the inherent quality of the beam (i. e., the transverse momentum due to the temperature of the plasma from which the ions are extracted), one can write¹

$$v = \frac{\beta \gamma \iint da_x dx}{\pi} = \beta \gamma E, \quad (4)$$

where v is the invariant, the integral is taken over the phase area ellipse at a particular energy, and β is the velocity measured in units of c , and γ , the total energy in rest mass units at the energy in question.

Experimental evidence on existing systems shows an approximate adherence to the rule

$$I = \pi v \delta \quad (5)$$

where I is the beam current and δ is a constant. Typical figures for present-day sources are $v = 0.3$ cm-mrad at $I = 100$ mA.

Buncher for dc Beam

In order to prevent damage to the linear accelerator, to reduce loading on the rf system, and to conserve beam, a buncher is used to improve the fraction of the dc beam captured by the linear accelerator. In its most primitive form, the buncher consists of (a) a single rf gap, properly phased, operating at the frequency of the linear accelerator, followed by (b) a drift space in which the accelerated and decelerated particles catch up or fall behind to coincide with the particles which crossed the buncher gap as the voltage was passing through zero. If we select as time zero the point at which the voltage is zero and rising, we can write, nonrelativistically, for the particle leaving the gap at a phase ϕ_0

$$v = v_0 + \Delta v \sin \phi_0 = v_0 \left(1 + \frac{1}{2} \frac{V}{E_0} \sin \phi_0 \right), \quad (6)$$

where v_0 and E_0 are the nominal velocity and kinetic energy of the dc beam, and V is the peak voltage on the buncher gap. The relative phase at subsequent times will be

$$\begin{aligned} \phi(t) &= \phi_0 - \frac{2\pi t}{\beta_0 \lambda} \Delta v \sin \phi_0 = \phi_0 - \pi \frac{V}{E_0} \frac{s}{\beta \lambda} \sin \phi_0 \\ &= \phi_0 - \xi \sin \phi_0, \end{aligned} \quad (7)$$

where s is the distance from the buncher to the first rf gap. The buncher parameters are contained in the quantity ξ . The limitations of this system are that the modulation voltage must be small compared to the energy error acceptable to the linac (linear accelerator), and large compared to the energy error in the dc beam. The practical performance by these devices improves the linac acceptance from about 20% to perhaps 60%. More complicated designs can improve the performance even more. Among these improvements are the utilization of the harmonics of the frequency to approximate a saw-tooth voltage wave on the gap or gaps.

Linear Accelerators

The 2π -mode standing-wave linear accelerator can be described as a succession of unit cells measured from the center of one drift tube to the center of the next. A unit cell is sketched in Fig. 4.

The perfect particle rides exactly at the synchronous phase ϕ_s and has a velocity β_s measured in units of c (the velocity of light).

The efficiency of the structure in accelerating the test particle (synchronous particle) is measured by the effective shunt impedance $\tilde{\Gamma}$,

$$\tilde{\Gamma} = \frac{(\xi_0)^2}{P_L}, \quad (8)$$

where P_L is the power lost in the structure per unit length; and ξ_0 is the effective accelerating field, and in turn is

$$\xi_0 = E_0 \dot{T} \quad (9)$$

with E_0 the peak axial electric field, and T , the transit-time factor, depends upon the geometry of the cell.

$$\begin{aligned} T &= \frac{\sin \pi g/L}{\pi g/L} \cdot \frac{I_0(K_1 \rho)}{I_0(K_1 a)}, \\ K_1 &= 2\pi \left[\left(\frac{1}{L} \right)^2 - \left(\frac{1}{\lambda} \right)^2 \right]^{1/2} \end{aligned} \quad (10)$$

$\lambda = c/f$ (the rf wavelength).

The first part measures the amplitude of the accelerating wave, and the I_0 's (Bessel functions of pure imaginary argument) measure the effectiveness of the drift tube in defining the geometry. At $\rho = a$, this factor is 1.

Shown in Fig. 5 are the variations of these parameters with the appropriate variable. The shunt impedance \tilde{r} is shown as a function of energy in Fig. 6.

The energy gain of the synchronous particle is given by

$$dW_s/dz = e \xi_0 \cos \phi_s . \quad (11)$$

It is notable that the efficiency of the acceleration drops off at both high- and low-energy ends. It is this feature and, more important, the practical matters of voltage holding and the bore size required to accommodate the beam that determine the energy of the dc injector. The practical choice for a linac operating at 200 mc/sec is between 500 and 750 keV, which is a convenient voltage to hold in air around the terminal of the Cockcroft-Walton. The loss in efficiency of the structure at the high-energy end of the scale would motivate one to change to a more efficient method of acceleration.

As pointed out previously, the transverse phase area decreases as acceleration through the linac proceeds, assuming the appropriate measures have been taken to contain the beam by focusing elements (see Appendix) in the drift tubes;^{3,4} further, the phase oscillation in longitudinal phase space damps and the momentum error decreases in the ideal machine.

For brevity we will simply state the laws for this damping.

$$\text{Transverse} \quad \alpha = p_x/p_z \propto \frac{1}{\beta\gamma} \quad (12)$$

$$\text{Longitudinal} \quad \Delta\phi \propto (\beta\gamma)^{-3/4} \quad (13)$$

$$\Delta p/p \propto \beta^{-5/4} \gamma^{-1/4} . \quad (14)$$

The wave length for a phase oscillation is given by

$$\lambda(\phi) = \left[\frac{2\pi \lambda_0 \gamma_s^3 \beta_s^3 m_0 c^2}{e \xi_0 (-\sin \phi_s)} \right]^{1/2} \propto (\beta_s \gamma_s)^{3/2} . \quad (15)$$

In practice, the errors in such things as the machine operating levels and misalignments will double or even triple the sizes that can be computed from Eqs. (12) through (14). Representative values for a beam at 50 MeV in existing 200 mc/sec linacs are ($\beta = 0.314$, $\gamma = 1.053$):

$$E = 3\pi \times 10^{-3} \text{ rad-cm and}$$

$$\Delta p/p = 3 \times 10^{-3}$$

$$\Delta\phi = \pm \pi/16 .$$

Debuncher

The desirability of reducing the momentum error between the linac output and injection into the synchrotron will become apparent in the next section when the rf requirements of the synchrotrons are described and space-charge limits are discussed. A simple system for accomplishing this is to allow the beam to drift until the initial momentum error $(\Delta p/p)_i$ causes the bunches to spread in phase, then to have them cross an rf gap or gaps phased so that the synchronous particle crosses when the voltage is zero and rising. The longitudinal extent of the bunch is small enough that only the approximately linear part of the sinusoidal voltage wave is used. The change in velocity of the extreme particles in a given bunch is

$$\Delta v = c\Delta\beta = \frac{2\beta_s c}{\gamma_s} \left(\frac{\Delta p}{p}\right)_i, \quad \Delta p \ll p, \quad \Delta\beta \ll \beta. \quad (16)$$

The time required for the phase to spread from $\Delta\phi_i$ to $\Delta\phi_f$ is

$$t = \frac{(\Delta\phi_f)}{\omega\Delta v} \beta_s c = \frac{(\Delta\phi_f) \gamma_s^2}{2(\Delta p/p)_i \omega}, \quad (17)$$

where $\omega = 2\pi f$. The final phase spread is given in terms of the drift distance l by

$$\Delta\phi_f = \frac{4\pi f (\Delta p/p)_i l}{\beta_s c \gamma_s} + \Delta\phi_i . \quad (18)$$

The voltage required for a specified reduction in momentum error is

$$\pm eV = \pm \left[\left(\frac{\Delta p}{p}\right)_i - \left(\frac{\Delta p}{p}\right)_f \right] \frac{m_0 c^2 \gamma_s \beta_s^2}{\sin \Delta\phi_f/2} . \quad (19)$$

Injector AG Synchrotron

The alternating-gradient magnet system of the synchrotron performs two functions: (a) it bends the equilibrium orbit into an approximate circle, and (b) it confines the beam in the vacuum chamber. The dimensions of the vacuum chamber and hence the costly magnet aperture are determined by a number of factors, including the desired admittance of the system. The orbits in an AG synchrotron describe a roughly sinusoidal path around the ring, whose wavelength is assumed large compared to individual magnet lengths;^{5,6} upon these orbits is superimposed a

wiggle or flutter which reflects the alternating-gradient structure of the magnet system. Computer programs are used to determine the values for the functions required to compute the aperture requirements for any given arrangement. The phase area of the synchrotron's admittance, written in terms of angle-displacement, is

$$A = \frac{\pi \nu a^2}{RF} = \frac{\pi a^2}{\beta_{\max}} \text{ rad-cm}, \quad (20a)$$

where ν is the number of betatron oscillations per revolution around the machine, a is the semiaperture (vertical or horizontal), and R is the radius of the machine. The quantity F is the form factor or flutter factor and measures the ratio of the maximum amplitude of the betatron oscillation β_{\max} to its average value β_{av} , hence

$$F = \beta_{\max} / \beta_{av} = \beta_{\max} / \frac{R}{\nu} = \beta_{\max} \nu / R > 1, \quad (20b)$$

$$\beta_{av} = R / \nu.$$

The angle of divergence acceptable to such a machine at injection is $\theta = a\nu/R$ radians, and this causes an amplitude of betatron oscillation of

$$x_{\max} = \left(\frac{RFA}{\pi \nu} \right)^{1/2} = \left(\frac{\beta_{\max} A}{\pi} \right)^{1/2}. \quad (21)$$

Synchrotron oscillations result from the radial displacement due to momentum errors in the injected beam and are given by

$$r_{\text{sync}} = a_p (\max) \Delta p / p, \quad (22)$$

where a_p is called the momentum compaction factor and is defined as

$$\frac{\Delta C}{C} \equiv a \frac{\Delta p}{p} \approx \frac{1}{\nu^2} \frac{\Delta p}{p}, \quad (23)$$

where C is the circumference of the machine. The above two oscillations show the space required for the beam emittance in a perfect machine. In addition to this, additional space is needed for errors in magnetic field, magnet alignment, and stray fields. Shown in Table I are the aperture requirements for an 8-BeV proton synchrotron to give an idea of the relative importance of error versus space required by the nature of the guide system and beam-phase area.

Table I. Aperture Requirements for 8-BeV Synchrotron.

	<u>cm</u>
Vertical	
x_{co} (closed-orbit deviation due to errors)	0.87
x_i (injection error in angle)	0.15
x_β (betatron oscillation amplitude)	1.44
Horizontal	
r_{co} (closed-orbit deviation due to errors)	0.96
r_i (injection error in angle)	0.37
r_β (betatron oscillation amplitude)	1.32
r_{sync} (synchrotron oscillation amplitude)	0.48

In Table I, $\Delta p/p$ is assumed to be 10^{-3} , $\nu_x = 10.25$, $\nu_r = 11.25$, $E = A = \pi \times 10^{-3}$ cm-rad at $E = 200$ MeV.

The value of the bending magnetic field on the equilibrium orbit at injection should be large compared to the values of stray fields around the ring and remnant fields in the magnet steel. The present AG machines inject at around 150 gauss, which is close to the lower limit, and in the machine above the injection field is about 500 gauss.

The momentum error at injection also determines the rf voltage requirements in the synchrotron; the rf bucket height required to equal the momentum error is

$$\pm eV = \left(\frac{\Delta p}{p} \right)_i^2 \frac{\pi h \eta p_i \beta c}{[(\pi - 2\phi_s) \sin \phi_s - 2 \cos \phi_s]} \quad (24)$$

where

$$h = \frac{\text{frequency of rf}}{\text{particle-revolution frequency}},$$

the harmonic order;

$$\eta = \left| 1/\gamma^2 - 1/\gamma_t^2 \right|,$$

γ = particle total energy in rest mass units

γ_t = transition energy $\approx \nu$;

ϕ_s = synchronous phase angle.

Since the rf power increases as the square of the voltage, the rf power requirements are dependent upon the fourth power of the momentum error.

The scheme envisioned for the machine discussed here allows the rf structure of the linac to wash out by drifting around the ring before it is adiabatically picked up at the starting frequency, f , of the synchrotron rf. The debunching

will take place in a time

$$t = \frac{1}{2\pi f_1} \frac{(2\pi - \Delta\phi)}{\eta \Sigma F/p} \quad (25)$$

The rf voltage should be slowly turned on and reach a value about twice or somewhat more than the voltage prescribed in equation (3). "Slowly" in this case means the order of time for a few phase oscillations which can be obtained from the circular frequency of phase oscillations.

$$\Omega = \frac{c}{R} \left(\frac{h \eta eV \cos \phi_s}{2\pi E} \right)^{1/2} \quad (26)$$

where E is the kinetic energy. The time required is $t = 2\pi/\Omega$.

Space Charge Limits

The final energy of the injector synchrotron depends upon considerations such as those sketched above, and the estimated limits of the amount of charge that could be accommodated by a vacuum chamber of given dimensions. The frequency of the betatron oscillations in the synchrotron is shifted by an amount either half-integral ($\Delta\nu = 1/2$) or quarter-integral ($\Delta\nu = 1/4$). A resonance may be crossed which can drive the entire beam into the vacuum-chamber wall. The particular resonance which is catastrophic depends on detailed analysis of the particular structure and how long one remains on the resonance. However, for our purposes and to obtain a rough idea of the limits imposed by the self force of the beam charges upon each other, we can write shift in ν caused by N protons which occupy a fraction B of the circumference (B is the bunching factor) where the beam has a cross-sectional area A ,

$$\Delta\nu = - \frac{N}{BA} \frac{e^2 R}{2\nu m_0 c^2 \beta^2 \gamma^3} \quad (27)$$

or

$$N \propto \beta^2 \gamma^3.$$

This shows a steep increase in the space charge limit as a function of injection energy. However, more sophisticated analysis than that leading to the above formula significantly modifies the results in certain cases.^{7,8,9} The space charge limit for higher energies and small apertures approaches $N \propto \gamma$.

Appendix

Radial Focusing in Linear Accelerators

An approximate treatment for an alternating-gradient radial-focusing system of the linear accelerator can be made by utilizing some of the concepts introduced in the preceding section on the synchrotron. The situation is different for the linear system in that there is a net defocusing force due to the rf acceleration and the orbit does not close. Further, the quadrupole lenses are placed in drift tubes whose spacing increases as the particles are accelerated, and hence the lens elements are not equal distances apart. The quasi-periodicity in the spacing of the lenses introduces no serious error in the estimated system so long as the spacing changes slowly compared to the wavelength of a betatron oscillation; this is a realistic assumption.

We have a series of quadrupoles (treated as thin lenses) spaced one or more cell lengths ($\beta_s \lambda$) apart and will assume a uniform bore diameter $2a$. As before, the phase area accepted by this system is

$$A = \frac{\pi a^2}{\beta_{\max}} \text{ rad-m,}$$

where lengths are measured in meters.

Above 50 MeV, a quasi-periodic system of doublets, consisting of (a) plus and minus quadrupoles in adjacent drift tubes followed by (b) a number of drift tubes without magnets, then (c) another pair of quadrupoles in adjacent drift tubes as shown in the sketch (Fig. 7) can be described approximately by the following relationships:

$$\beta_{\max} = \frac{1}{\sin \mu_r} (\Delta \text{ch } \phi_r + \frac{n L \text{ sh } \phi_r}{\phi_r})$$

with

$$\phi_r = \left(\frac{\pi e \xi_0 \cos \phi_s}{m_0 c^2 \lambda \beta^3 \gamma^3} \right)^{1/2} nL.$$

The approximate strength of the quadrupoles is given by

$$G = \frac{p}{e} \left(\frac{\delta}{\ell^2 \Delta} \right)^{1/2},$$

with ℓ the length of the quadrupole, Δ the distance between the elements of the doublet, and

$$\delta = \frac{2 \phi_r}{n L \text{ sh } \phi_r} (\text{ch } \phi_r - \cos \mu_r).$$

The emittance of existing 200 mc/sec linacs at 50 MeV is

$$A = 30\pi \times 10^{-6} \text{ rad-m.}$$

The other parameters pertinent here are

$$n = 3$$

$$\beta_s = 3.14 \times 10^{-1}, \gamma_s = 1.053$$

$$\frac{p}{e} = \frac{3.1 \times 10^8 \text{ eV/c}}{c} = \frac{3.1 \times 10^8}{3 \times 10^8} \text{ m/sec}$$

$$e \xi_0 = 1 \text{ MeV/m}, \lambda = 1.5 \text{ m}$$

$$\phi_r = 0.114$$

$$\beta_{\text{max}} = 2$$

$$a \approx 0.776 \text{ cm}$$

$$G = 10 \text{ tesla/m} = 1000 \text{ G/cm.}$$

Utilizing a phase advance per cell of the betatron oscillation of $\pi/2$, we see that $\sin \mu_r = 1$ and $\cos \mu_r = 0$. Below 50 MeV, and particularly at the low-energy end of the machine, the focusing requirements are more severe, but the problem has been solved in existing machines.

References

1. A. Van Steenberg, "Beam Current Limitations in the AGS with Multiple Turn Injection Related to Ion Source Emittance Characteristics," Accelerator Department, Brookhaven National Laboratory Internal Report AADD-29; 1964.
2. Lloyd Smith, "Orbit Considerations in the Linear Accelerator," Accelerator Development Department, Brookhaven National Laboratory Internal Report LS-3; 1961.
3. Lloyd Smith, "Linear Accelerators," Encyclopedia of Physics, Springer Verlag, Berlin, Vol. XLIV, pp. 341-389; 1959.
4. Lloyd Smith and Robert L. Gluckstern, "Focussing in Linear Ion Accelerators," Rev. Sci. Instr., Vol. 26, No. 2, pp. 220-228; February 1955.
5. G. K. Green and E. D. Courant, "The Proton Synchrotron," Encyclopedia of Physics, Springer Verlag, Berlin, Vol. XLIV, pp. 218-341; 1959.
6. M. Stanley Livingston and John P. Blewett, "Particle Accelerators," McGraw-Hill, N. Y., pp. 581-614; 1962.

7. L. J. Laslett, "On Intensity Limitations Imposed by Transverse Space Charge Effects in Circular Particle Accelerators," Proceedings of the Summer Study on Storage Rings, Accelerators and Experimentation at Super-High Energies, Brookhaven National Laboratory Report BNL-7534, pp. 324-367; 1963.
8. L. J. Laslett, V. Kelvin Neil, and Andrew M. Sessler, "Transverse Resistive Instabilities of Intense Coasting Beams in Particle Accelerators," Lawrence Radiation Laboratory Report UCID-11090, Rev. 1; November 1964.
9. V. Kelvin Neil and Andrew M. Sessler, "Longitudinal Resistive Instabilities at Intense Coasting Beams in Particle Accelerators," Lawrence Radiation Laboratory Report UCID-11089; September 1964.

Figure Captions

Fig. 1. Diagram of injection system for 200-BeV proton synchrotron.

Fig. 2. Aperture system defining transverse phase space.

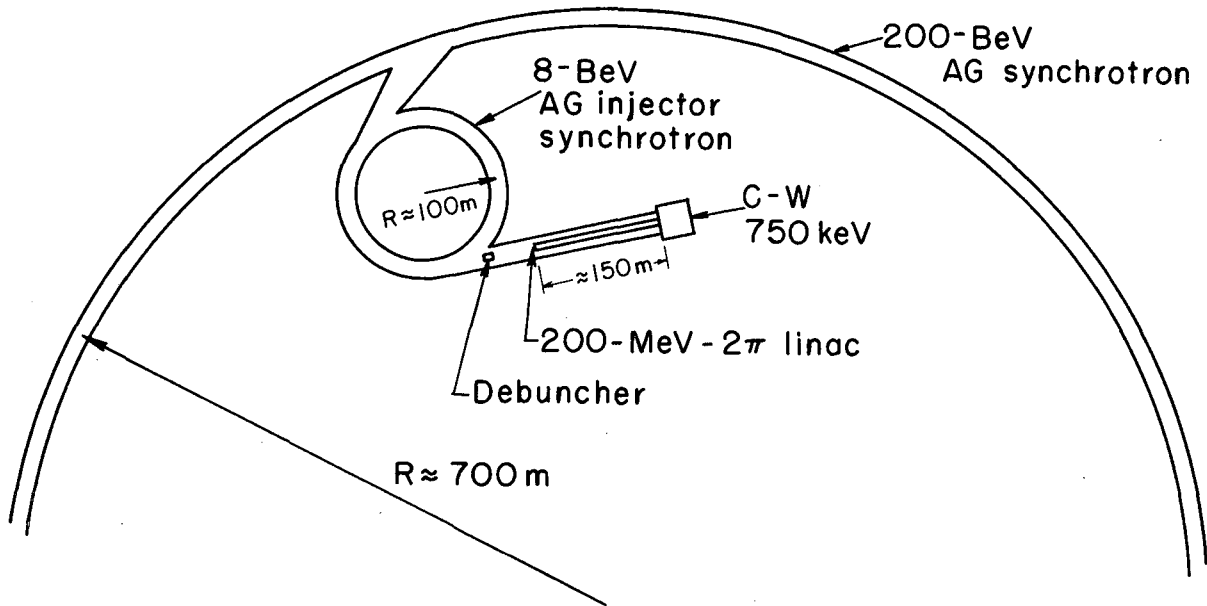
Fig. 3. Phase space area behavior.

Fig. 4. Unit cell of 2π linear accelerator.

Fig. 5(a). Transit-time factor on axis as a function of a .
(b). Transit-time factor as a function of g/L .

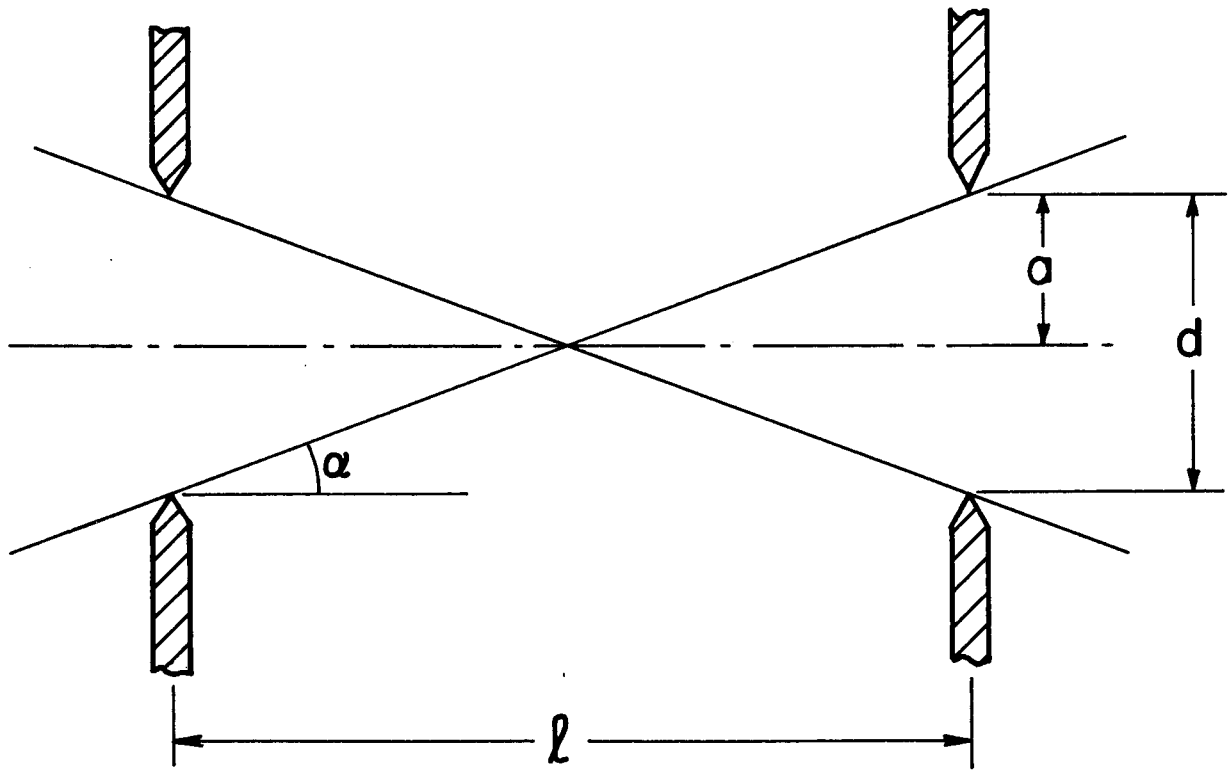
Fig. 6. Shunt impedance of 2π linac structure as a function of β .

Fig. 7. Diagram of doublet focusing system.



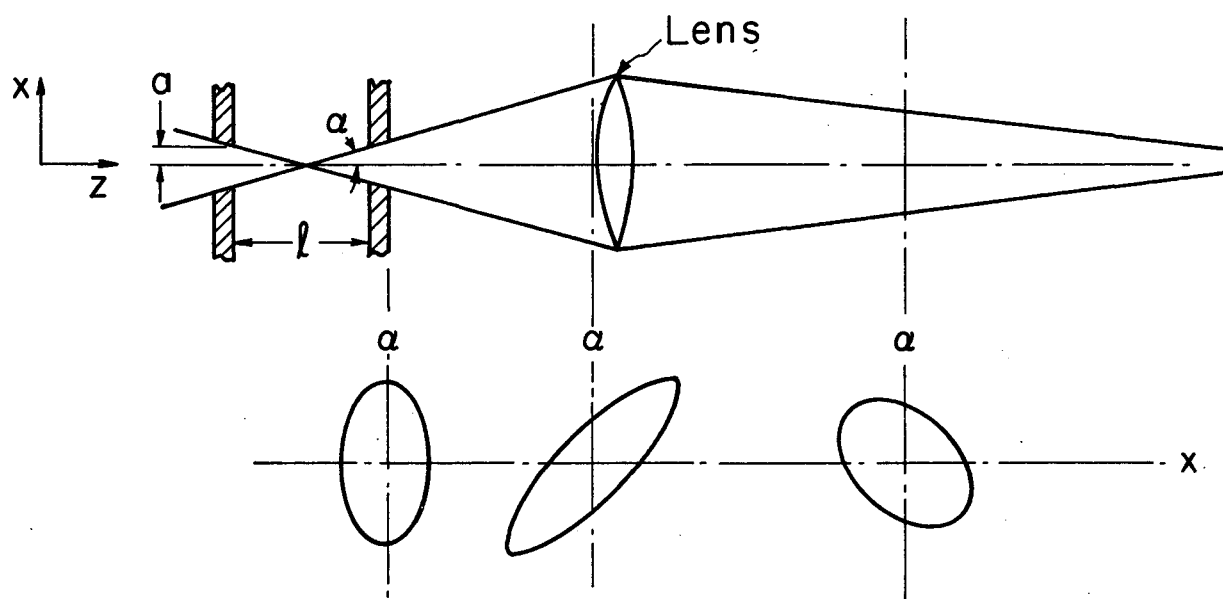
MUB-5320

Fig. 1



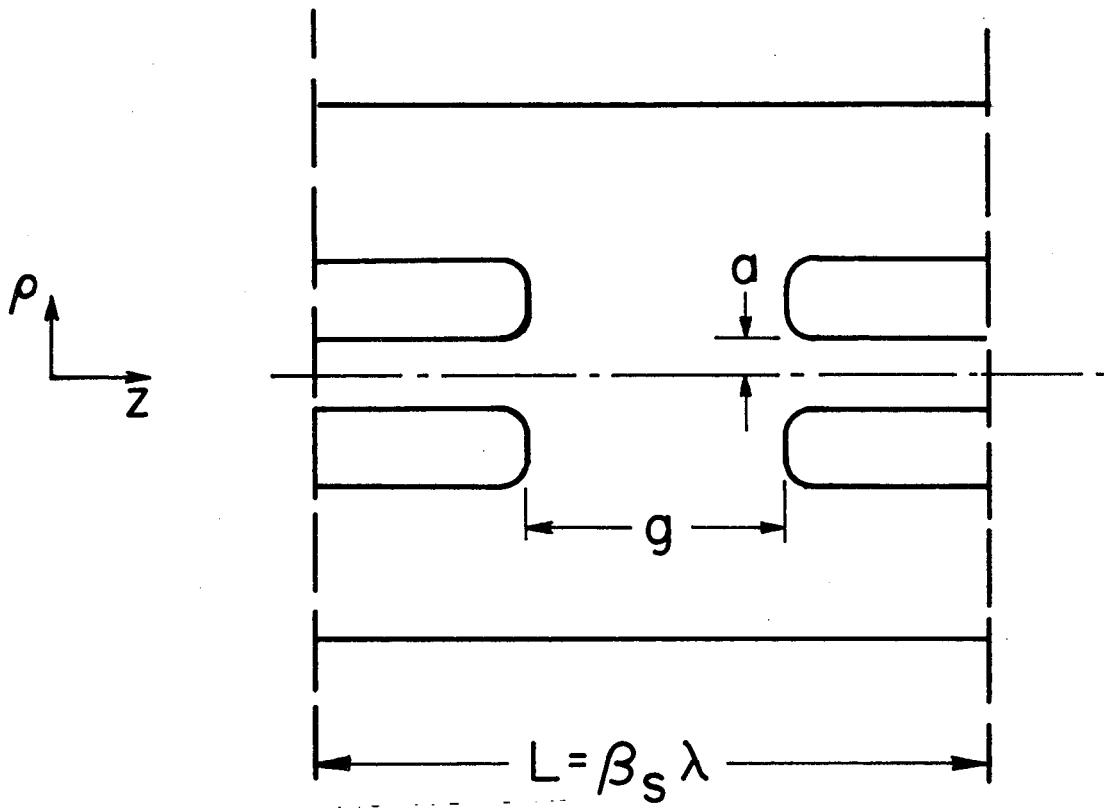
MUB-5321

Fig. 2



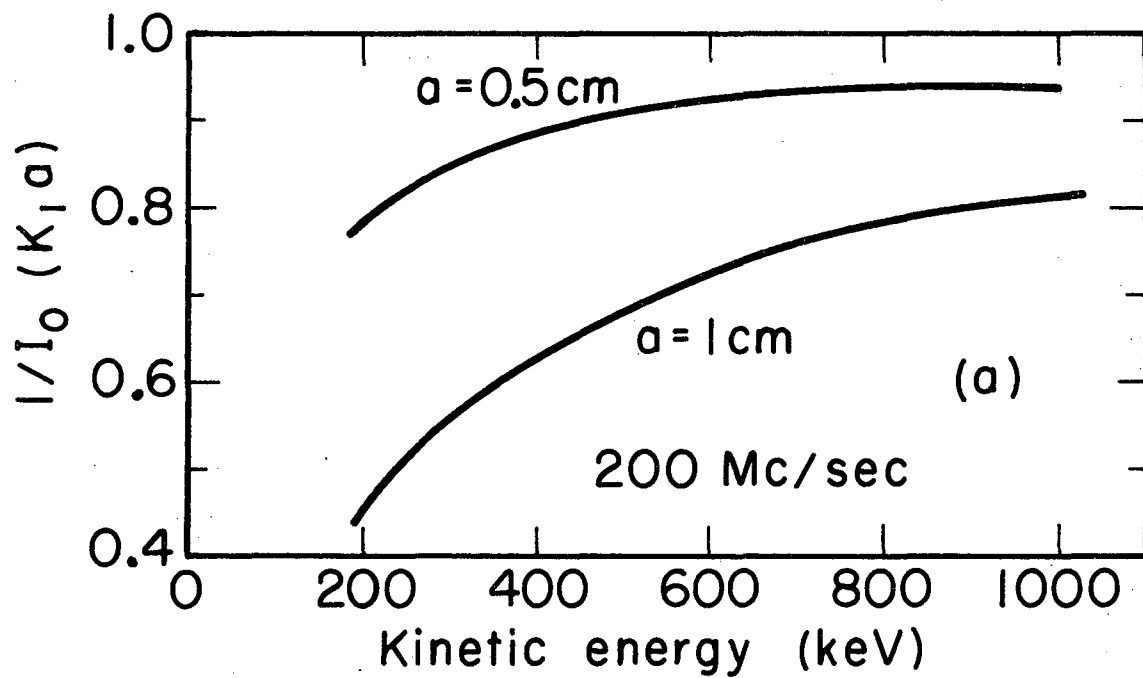
MUB-5322

Fig. 3



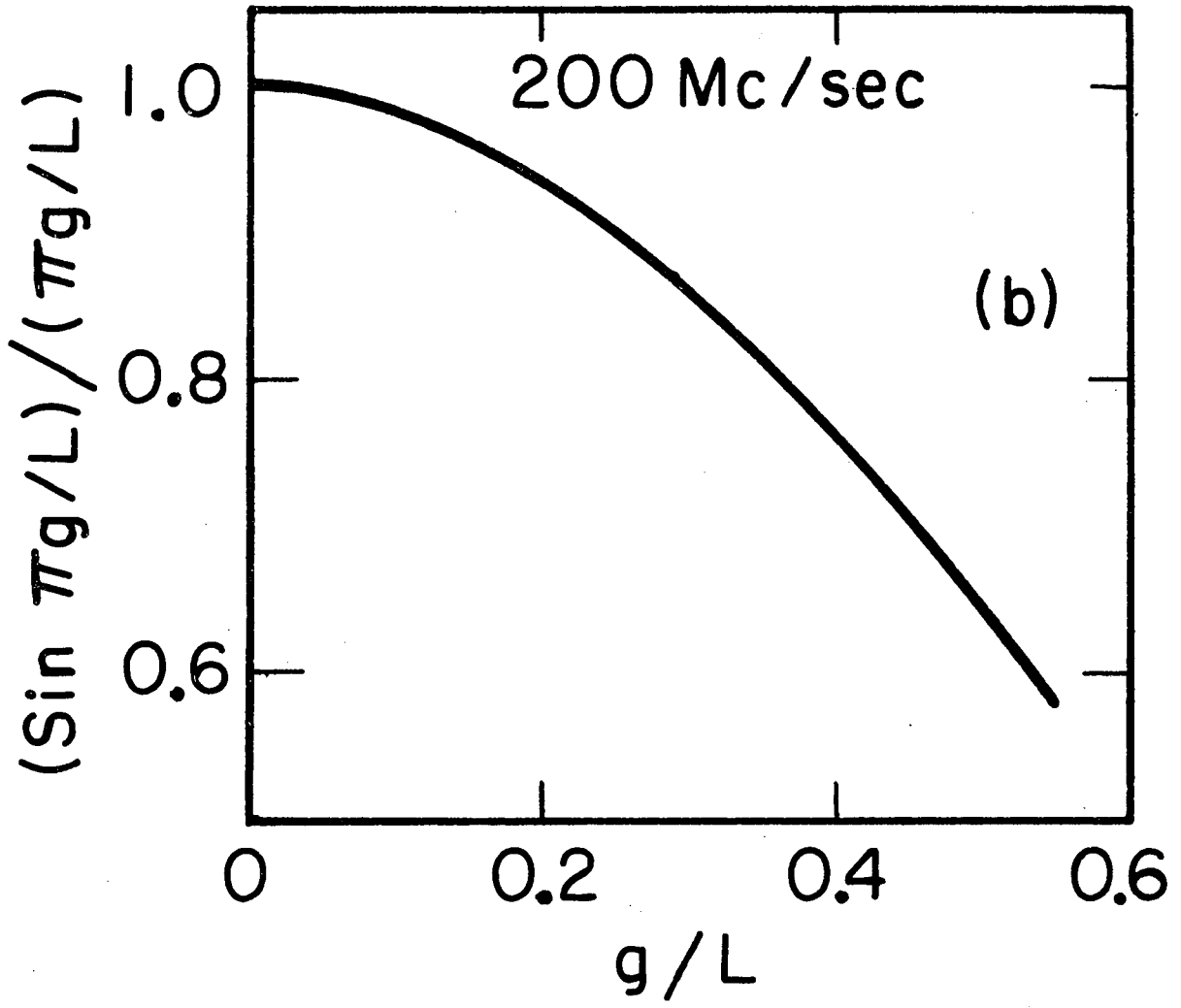
MUB-5323

Fig. 4



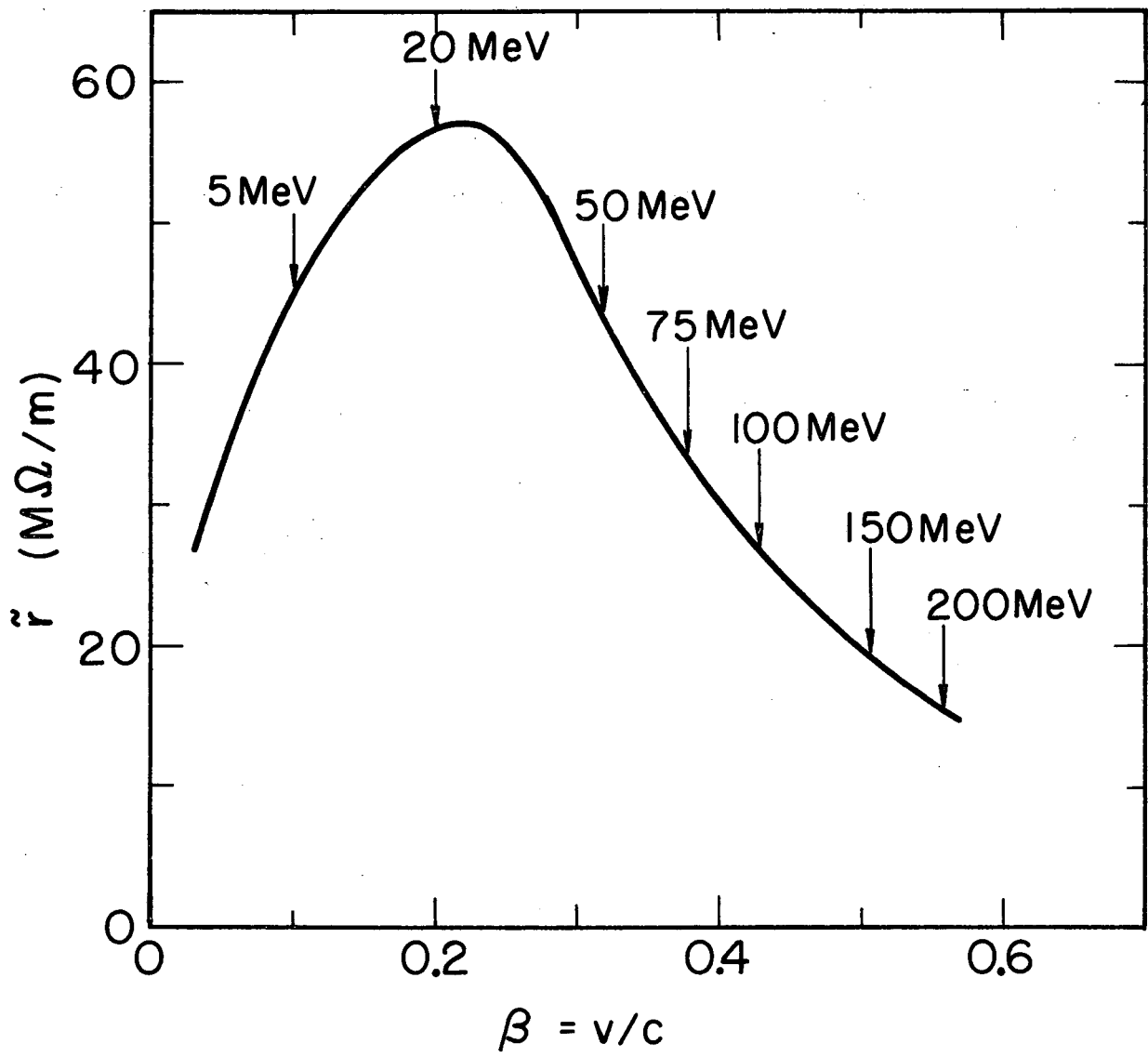
MUB-5324

Fig. 5a



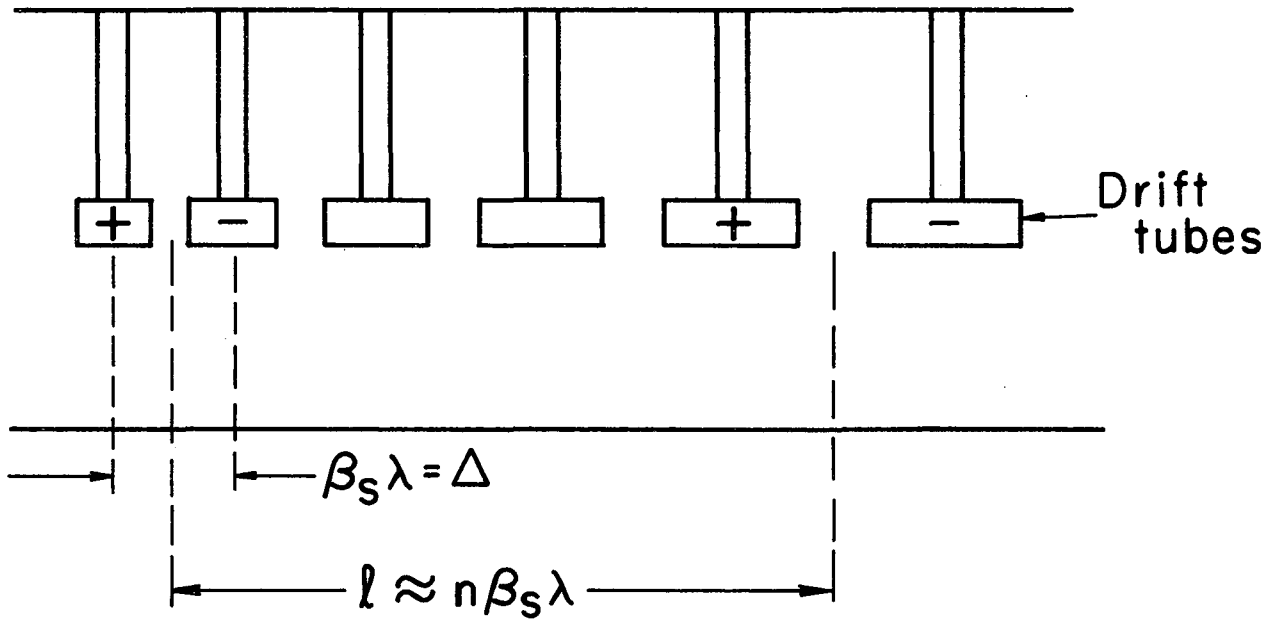
MUB-5325

Fig. 5b



MUB-5326

Fig. 6



MUB-5327

Fig. 7

This report was prepared as an account of Government sponsored work. Neither the United States, nor the Commission, nor any person acting on behalf of the Commission:

- A. Makes any warranty or representation, expressed or implied, with respect to the accuracy, completeness, or usefulness of the information contained in this report, or that the use of any information, apparatus, method, or process disclosed in this report may not infringe privately owned rights; or
- B. Assumes any liabilities with respect to the use of, or for damages resulting from the use of any information, apparatus, method, or process disclosed in this report.

As used in the above, "person acting on behalf of the Commission" includes any employee or contractor of the Commission, or employee of such contractor, to the extent that such employee or contractor of the Commission, or employee of such contractor prepares, disseminates, or provides access to, any information pursuant to his employment or contract with the Commission, or his employment with such contractor.

